

Design of a frictionless magnetorheological damper with a high dynamic force range

Ondřej Macháček , Michal Kubík, Zbyněk Strecker ,
Jakub Roupec and Ivan Mazůrek

Advances in Mechanical Engineering
2019, Vol. 11(3) 1–8
© The Author(s) 2019
DOI: 10.1177/1687814019827440
journals.sagepub.com/home/ade
 SAGE

Abstract

This article discusses an increase in dynamic force range in a spring–damper unit achieved by elimination of sealings' friction. This friction is a part of damping force that cannot be controlled; therefore, it is undesirable in magnetorheological dampers. A new design of a magnetorheological damper with no friction force is described and compared with a traditional magnetorheological damper consisting of a piston and piston rod seals. In the traditional design, fluid is forced to flow by a hydraulic cylinder with high friction caused by sealings. In order to eliminate this friction, a frictionless unit made of metal bellows was designed. Elastic metal bellows can be sealed only by static seals. The measurement of force–velocity dependency was carried out for the original and the new damper with the same magnetorheological valve. The results indicate that the frictionless unit exhibits a significant improvement in the dynamic force range. In the case of adaptive-passive damping control, the increase in the dynamic force range enables the improvement of vibration elimination in the entire frequency range.

Keywords

Magnetorheological damper, frictionless, dynamic force range, metal bellows, transfer ratio

Date received: 4 April 2018; accepted: 7 January 2019

Handling Editor: ZW Zhong

Introduction

Vibrations – an accompanying feature of movement – are generally undesirable. There are several ways of how to reduce them. The commonly used passive dampers do not need any power supply; however, they are not very efficient, as it is not possible to achieve good damping in a wide frequency range with a single damper. Another way of how to eliminate vibrations is using an active element – actuator. This suspension is better in vibration elimination especially at low frequencies, but it is energy consuming. Therefore, active suspension systems are used specifically for light sprung masses.¹ Semi-active damping is often referred to as an advantageous combination of passive and active vibration elimination.² However, the method of semi-active damping is more similar to that of passive damping

because both methods are based on the reduction of vibration energy within the system,³ while the active control adds the energy to the system. Semi-active damping differs from the passive one in controllability of dissipated energy in the damper. Magnetorheological (MR) damper is one of the examples of such devices. Usually, it consists of a piston with the coil that can generate the magnetic field in the active zone.^{4,5} However, there are several designs of MR dampers

Institute of Machine and Industrial Design, Brno University of Technology, Brno, Czech Republic

Corresponding author:

Ondřej Macháček, Institute of Machine and Industrial Design, Brno University of Technology, Technická 2896/2, 61669 Brno, Czech Republic.
Email: Ondrej.Machacek@vutbr.cz



Creative Commons CC BY: This article is distributed under the terms of the Creative Commons Attribution 4.0 License (<http://www.creativecommons.org/licenses/by/4.0/>) which permits any use, reproduction and distribution of the work without further permission provided the original work is attributed as specified on the SAGE and Open Access pages (<https://us.sagepub.com/en-us/nam/open-access-at-sage>).

consisting of the piston unit and the external MR valve.^{6,7} This type of damper has to be filled with an MR fluid – a smart material consisting of micro- or nano-sized ferromagnetic particles, a carrier fluid and some additive ingredients.⁸ When this fluid is exposed to the magnetic field, its yield stress dramatically raises, which increases damping forces.^{9,10}

Figure 1(a) shows the example of a suspension system with a vibrating base and sprung mass. One of the main aims of this suspension system is to minimize the vibrations transferred from the base to the sprung mass, that is, to keep the transfer ratio a_1/a_0 between the base and the sprung mass as low as possible. The elimination of vibrations can be divided into two areas by frequency as follows: vicinity of resonance and isolation.¹¹ The increase in the damping ratio causes a lower transfer in the vicinity of resonance

$$\frac{\omega}{\omega_n} \leq \sqrt{2} \quad (1)$$

where ω represents the frequency of excitation and ω_n represents the natural frequency of the system. On the other hand, an increase in damping causes also the increase of the transfer ratios for the isolation area in the frequency range

$$\frac{\omega}{\omega_n} > \sqrt{2} \quad (2)$$

Therefore, it is reasonable to adapt the damping for current frequency of excitation. The adaptive-passive damping control is one of the suitable methods for elimination of vibrations with harmonic excitation.¹² It is based on variable damping in time, high damping in the vicinity of resonance (equation (1)) and low damping for isolation area (equation (2)).¹³ Yang et al.⁵ proved that the semi-active suspension with an MR damper with a high dynamic force range and a short response time is very efficient in vibration elimination. The response time is an interval necessary to change the damping ratio.¹⁴ The time period of this change depends on the fluid response time, coil inductance and eddy currents in the magnetic circuit.¹⁵ Currently, the world's fastest MR damper with response time less than 2 ms was developed by Strecker et al.¹⁶

Dynamic force range of an MR damper

Generally, the greater the possibility of intervention in the system, the more effective regulation can be achieved.¹⁷ The dynamic force range of an MR damper (equation (3)) depends on the damper piston velocity, which can be calculated as the ratio of the damping force in the activated state F_{on} and the force in the inactivated state F_{off} of the damper. The OFF state force can be determined as the sum of forces caused by the

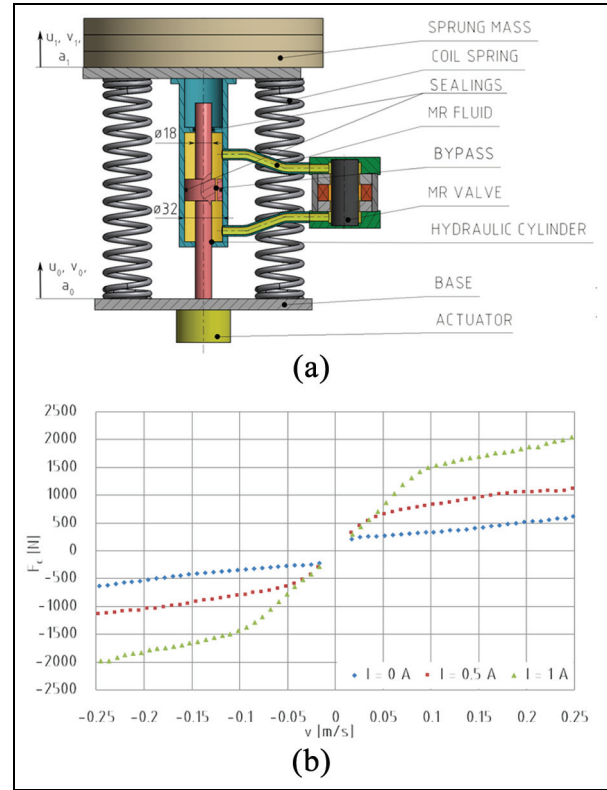


Figure 1. (a) Scheme of the suspension system and (b) force-velocity dependency of the MR damper with piston.

flow of the viscous fluid F_n and the friction F_f . The force caused by yield stress F_τ must be added to the sum of the ON state force. A dynamic force range is determined by the equation defined by Yang et al.⁵ and confirmed by Bai and Wereley¹⁸

$$D(v) = \frac{F_{on}(v)}{F_{off}(v)} = \frac{F_\tau + F_n(v) + F_f}{F_n(v) + F_f} = 1 + \frac{F_\tau}{F_n(v) + F_f} \quad (3)$$

Several methods of dynamic force range increase have been described. Yang et al.⁵ optimized the geometry of gap and piston. Cvek et al.¹⁹ chose the fluid that exhibits the greatest differences between the yield stress in the ON and OFF states. The influence of sealing friction has not yet been directly described in the available literature. However, it can be observed from Table 1 that the friction force could be a significant part of the damping force in the inactivated state, especially for the dampers with a low damping force.

The original MR damper with a piston

Two dampers with the same external MR valve are discussed in this study. The MR valve design is mentioned in our previous study,²¹ which deals among other things

Table 1. Forces and dynamic force ranges of the chosen MR dampers.

| Authors | F_{on} | F_{off} | F_f | D |
|---------------------------------|----------|-----------|---------|-----|
| Yang et al. ⁵ | 164 kN | 15.97 kN | 6.34 kN | 10 |
| Koo et al. (Lord) ¹⁴ | 1000 N | 180 N | 100 N | 5.6 |
| Wang et al. ²⁰ | 65 N | 32 N | 25 N | 2 |

MR: magnetorheological.

with F – v dependency prediction by an analytical model and its verification. In the first version of the MR damper, the fluid was forced to flow through the MR valve by a commercially available hydraulic cylinder. Seals are placed between the cylinder and the piston or the piston rod. These seals are the most significant cause of friction force that decreases a dynamic force range of an MR damper. The sprung mass was connected with the base by the coil spring and the damper; see Figure 1(a). This configuration is called a rigidly connected damper²² and the absolute transmissibility of the system with a constant damping ratio ξ is

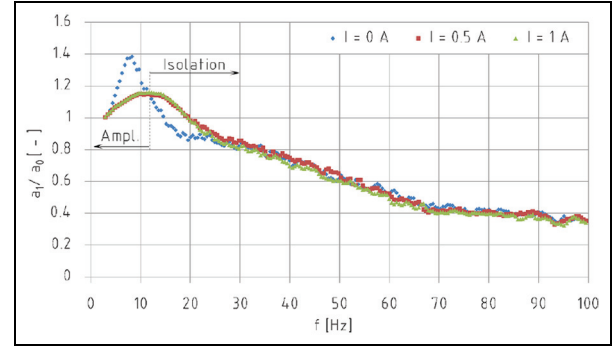
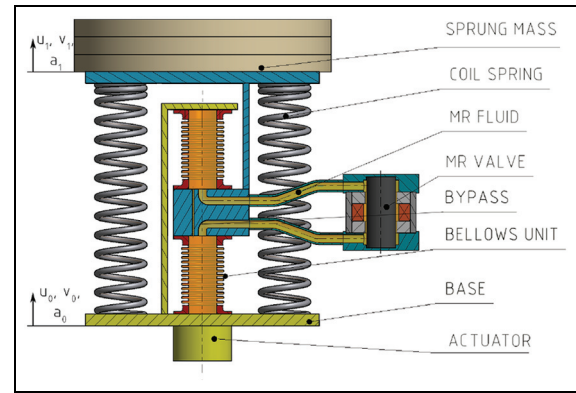
$$T(f) = \frac{a_1}{a_0} = \sqrt{\frac{1 + \left(2 \cdot \xi \cdot \frac{\omega}{\omega_n}\right)^2}{\left(1 - \frac{\omega^2}{\omega_n^2}\right)^2 + \left(2 \cdot \xi \cdot \frac{\omega}{\omega_n}\right)^2}} \quad (4)$$

However, the damping force F_c can be controlled by an electric current in the coil of the external MR valve, so the damping ratio is not constant. Thus, equation (4) is valid only in a limited range, for example, $I = 1$ A at $v = 0 - 0.08$ m/s. Force–velocity dependency of the original MR damper with a piston is shown in Figure 1(b).

Problem formulation

The efficiency of semi-active or adaptive-passive suspension depends on the dynamic force range of the MR damper (equation (3)). Due to the Coulomb friction, the dynamic force range of the MR damper with a piston is insufficient, especially for small piston velocities, which is confirmed by very small differences in the transfer ratios for different currents in the coil of the MR damper with a piston, particularly for frequencies higher than 30 Hz; see Figure 2.

The adaptive-passive damping control will be used in this study. It is necessary to minimize the forces in the OFF state to achieve a lower transfer ratio of the suspension system in the isolation area. The friction is a component of the OFF state force that can be changed without significantly affecting the ON state in an undesirable way. The friction in the traditional damper is caused especially by the sealing of surfaces with the motion relative to each other. The friction force depends on the pressure of the fluid inside the damper. The higher the

**Figure 2.** Transfer ratio of suspension with the MR damper with a piston.**Figure 3.** The suspension system with the MR damper with bellows.

pressure, the higher the downforce on the sealing, thus the higher the friction force.²³ However, commonly the friction force is considered to be constant for various velocities of the piston.⁴ Heipl and Murrenhoff²⁴ reduced this resistance using proper seals; however, the friction force was still significant. The friction can be completely eliminated using the bellows with static seals.^{25,26} Elastic metal bellows change the connection of the damper from rigidly to elastically connected; this change should reduce a transfer of vibrations at high frequencies.²⁷ This hypothesis needs to be verified for the suspension parameters mentioned in this study.

Material and methods

The new MR damper with bellows

Friction is eliminated by the absence of piston and piston rod and thus its sealing as well; see Figure 3. Sealing is achieved using elastic metal bellows which are sealed with static seals.

The structural modification regarding the absence of piston and piston rod cause a change in the dynamic behaviour of the system in comparison with the system

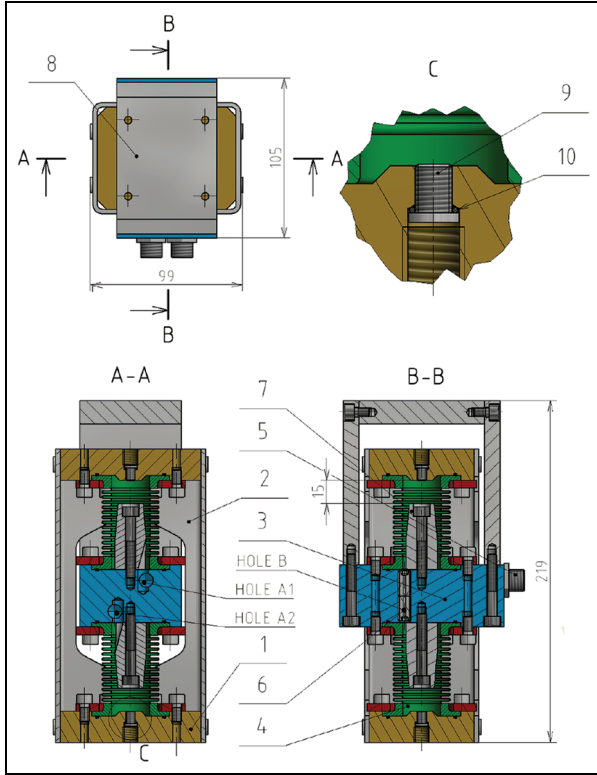


Figure 4. A detailed scheme of the bellows unit.

with the original damper because a new damper has to be considered elastically connected. In this case, the transmissibility of the system is

$$T(f) = \frac{a_1}{a_0} \sqrt{\frac{1 + 4 \cdot \left(\frac{N+1}{N}\right)^2 \cdot \xi^2 \cdot \frac{\omega^2}{\omega_n^2}}{\left(1 - \frac{\omega^2}{\omega_n^2}\right)^2 + \frac{4}{N^2} \cdot \xi^2 \cdot \frac{\omega^2}{\omega_n^2} \cdot \left(N + 1 - \frac{\omega^2}{\omega_n^2}\right)^2}} \quad (5)$$

where $N = k_1/k$ is the ratio between the stiffness of the damper connection k_1 and the axial stiffness of the system k . Equation (5) is valid for a linear system, and therefore equation (4) as well is valid only for constant current in the coil and a limited range of velocity.

Lids of the new damper (pos. 1) in Figure 4 are connected by a frame (pos. 2). Considering that the central part (pos. 3) is fixed, a downward movement of the frame causes compression of the upper bellows, while the lower bellows (pos. 4) is expanded. The length change of bellows caused the MR fluid flow via two channels. The first one is through the hole marked A1 and then through the fitting (pos. 5) and the pipes to the external MR valve and then back to the bellows unit through hole A2. The second channel is directly

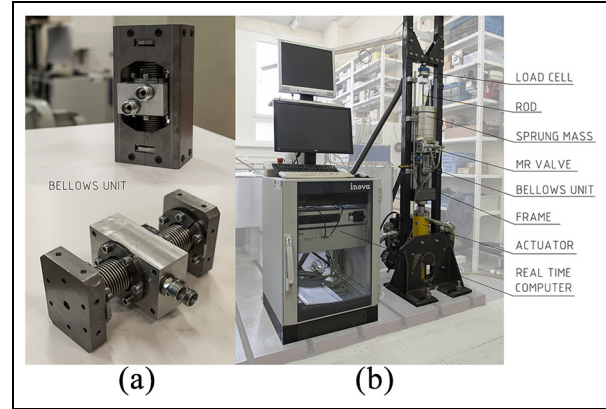


Figure 5. The bellows unit (a) in the test rig (b).

through the bypass hole B which is drilled in two plugs (pos. 6). The stopper (pos. 7) prevents the metal bellows from excessive deformation.

The bellows unit can be screwed to the weights and the actuator via threaded holes in the frame (pos. 8) and in the lid (pos. 1). This connecting hole in the lid can also be used for filling the fluid. It is sealed with the screw (pos. 9) and the O ring (pos. 10), and it is tightened to a conical countersink. This is an unconventional method of sealing; therefore, a leakage test was performed prior to manufacturing of the lids.

Measurement setup of force–velocity dependency

The MR damper with bellows shown in Figure 5(a) was mounted into the test rig as illustrated in Figure 5(b). The system parameters as sprung mass $m = 106.3$ kg and spring stiffness $k = 330$ N/mm were similar to those of the system with a piston unit. The sprung mass was connected with the actuator only by the coil spring and one of the examined MR dampers. The sprung mass can move only in vertical directions due to linear bearing in the case of the transfer ratio measurement. On the other hand, when the force–velocity dependency was measured, the sprung mass was fixed to the frame by a rod.

The damping force was measured with a strain gauge load cell INTERFACE 1730ACK-50 kN mounted between the sprung mass and the frame. The stroke of movement u was measured by a sensor integrated into the actuator INOVA AH 40-150 M56 and the velocity v was calculated from the signal of the stroke. Excitation was provided by the actuator which moves according to a linear sweep sine function with the frequency of 0.1 – 8 Hz and the amplitude of 5 mm. The actuator was set so that the springs were not preloaded for zero stroke. The force–velocity dependency is created from the points with zero stroke; see Figure 6. Therefore, the spring forces were eliminated in the force–velocity dependency. The system was filled with

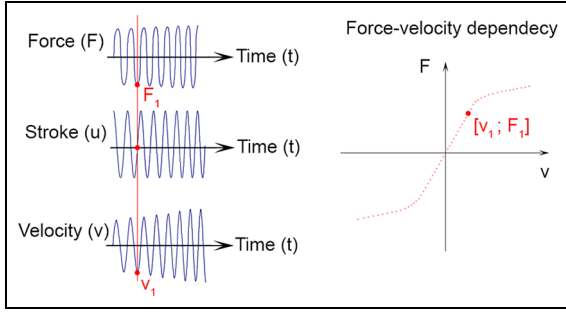


Figure 6. Scheme of force–velocity dependency measurement.

MRF 132 DG produced by LORD company. The bypass (hole B) had a diameter of 1.45 mm.

Measurement setup of the transfer ratios

The setup of this type of measurement was the same as that for the force–velocity measurement, only the load cell was removed and the actuator acceleration a_0 and the sprung mass acceleration a_1 were measured by two piezoelectric accelerometers of type B&K 4507B. The transfer ratio of the system was counted using the signals from both accelerometers which were converted to the frequency domain using fast Fourier transform (FFT). The amplitudes of both signals were divided for each frequency component

$$T(f) = \frac{a_1(f)}{a_0(f)} \quad (6)$$

Kinematic excitation was realized by linear sweep sine for frequencies from 3 to 100 Hz with constant amplitude of acceleration $1g = 9.81 \text{ m s}^{-2}$. The measurement of the transfer ratio was provided for three various values of electric currents in coil: 0, 0.5 and 1 A. The current was constant throughout the measurement for passive control. However, when the adaptive-passive control was used, the current I was switched according to the frequency of excitation f

$$\frac{2 \cdot \pi \cdot f}{\sqrt{\frac{k}{m}}} \leq \sqrt{2} \rightarrow I = 1 \text{ A} \quad (7)$$

$$\frac{2 \cdot \pi \cdot f}{\sqrt{\frac{k}{m}}} > \sqrt{2} \rightarrow I = 0 \text{ A} \quad (8)$$

Results and discussion

Force–velocity dependency of the MR damper with bellows

Force–velocity dependency of the MR damper with bellows in Figure 7 differs from the MR damper with a

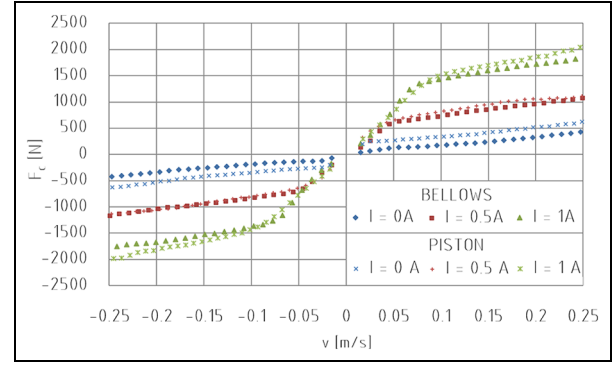


Figure 7. Force–velocity dependency of the MR damper with bellows.

piston in Figure 1(b), especially for the current of 0 A due to the friction elimination.

However, friction also affects the states with non-zero currents in the coil; therefore, the damping forces of the MR damper with bellows are lower than the forces of the MR damper with a piston. The slope of the measured curves is slightly different for both dampers; this is caused by different piston areas. Traditionally, it is given by a diameter of piston $D_p = 32 \text{ mm}$ and piston rod $d_r = 18 \text{ mm}$ (Figure 1). Nevertheless, the MR damper with bellows has no piston; therefore, the mean diameter $D_b = 30.25 \text{ mm}$ of bellows waves was considered for the calculation of the effective area. A presumption that the mean diameter can be considered as a virtual piston diameter was verified by measurement of the bellows load force and the pressure of the fluid inside the bellows. The effective areas of both pistons were slightly different because the offer of commercially available bellows and cylinders' manufactured dimensions is limited. However, this difference has a minimum impact on the dynamic force range.

Force–velocity dependencies of both dampers differ also by the hysteresis because of the different stiffness of the damper connection k_1 ; see Figure 8. The friction of the damper with the piston causes a force lag (horizontal segments at $F = 2000 \text{ N}$ or $F = -2000 \text{ N}$ at low piston velocities) which causes that the blue curve for the lowest velocity has not maximum force at velocity 0 m/s . This lag was not observed in the frictionless MR damper with bellows. Six points for each damper were used from the loops shown in Figure 8 for the force–velocity dependency determination by the method described above. The points are marked by circles and placed at the maximum and minimum velocities, thus at zero stroke, where the springs are not preloaded.

Transfer ratios of the MR damper with bellows

A resonance of the suspension system with the MR damper with bellows and no current in the coils of the MR valve is around 9 Hz, see Figure 9. A rise of the

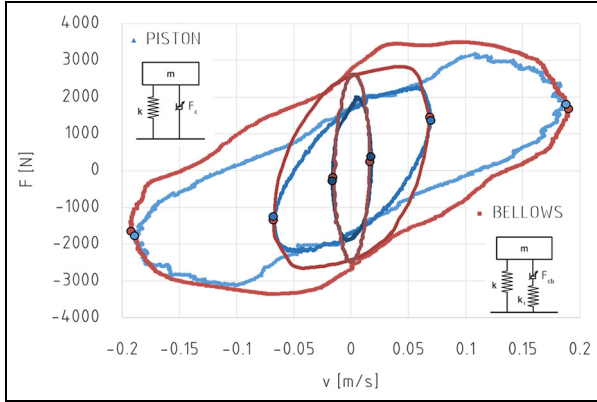


Figure 8. Comparison of force–velocity dependencies of both MR dampers with hysteresis caused by the springs.

current significantly reduces the transfer ratio (a_1/a_0) in the vicinity of resonance and moves the resonance to a slightly higher frequency up to the current $I = 0.5$ A. The current rise over 0.5 A increases the height of the resonance peak and also the resonance frequency; this trend corresponds to Brennan et al.²⁸ It is caused by the force ratio between the spring k_1 and the damper c connected in series, and the force ratio depends on the excitation frequency.

There are few small peaks in the transfer ratios between 50 and 60 Hz for all measurements. This is caused by natural frequencies of individual parts of the test rig. Resonance around 80 Hz with no current in the coil (blue curve) is presumably caused by MR fluid oscillation. Bellows are not rigid so the fluid with certain mass behaves as an oscillating rigid body on the spring k_1 and flows from one bellows to another. This is called a fluid mass effect.²⁷ The peak around 80 Hz disappears at higher currents in the coil because the magnetic field prevents the MRF from flowing through the MR valve; thus, the mass of the flowing fluid dramatically decreases and a small diameter of bypass hole causes higher damping (Figure 4 – hole B).

Benefits of the new MR damper with bellows

Both the above-mentioned dampers were compared in terms of the dynamic range and the transfer ratio of suspension systems with these dampers. The dynamic range $D(v)$ of the MR damper can be determined using equation (3). In this case, it is a ratio between the damping force with maximum current in the coil $I_{max} = 1$ A and no current in the coil $I_{min} = 0$ A. The dependency of the dynamic range and velocity is shown in Figure 10.

It is obvious that the MR damper with the bellows unit has a higher dynamic range for the entire velocity range in comparison with the MR damper with piston.

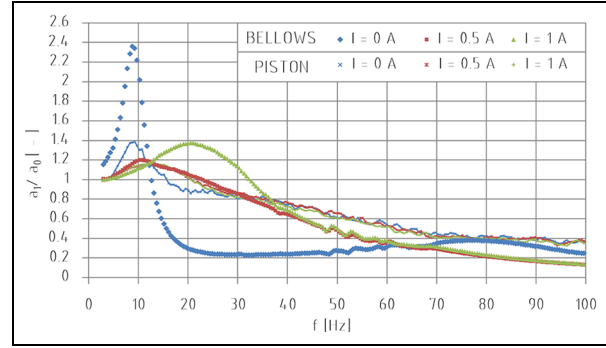


Figure 9. Transfer ratio of suspension with the MR damper with bellows.

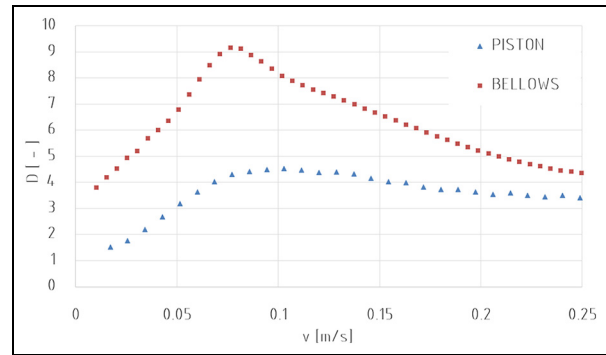


Figure 10. Comparison of the dynamic range.

The increase of the dynamic range is more than 100% for the velocity lower than 0.08 m/s.

Comparison of the transfer ratios of adaptive-passive controlled MR dampers is shown in Figure 11(a). The results show that the MR damper with bellows exhibits a lower transfer ratio in the whole frequency range than the transfer ratio of the MR damper with a piston. A new design of the damper with bellows affects the connection of the damper.

The MR damper with a piston can be considered as rigidly connected, while the MR damper with bellows is elastically connected²² because the bellows change their volume as a function of fluid pressure inside them. Davis et al.²⁷ call this resistance of bellows against the volume changes called as volumetric stiffness, which is a key parameter of the stiffness of frictionless damper connection k_1 . The results of stiffness k_1 measurement were approximately seven times higher than those of the spring stiffness k . The advantage of an elastically connected damper for current $I = 0.5$ A can be clearly seen in Figure 11(b). The transfer ratio of the elastically connected damper is lower than that of the rigidly connected damper for frequencies higher than 30 Hz and almost the same for frequencies lower than 30 Hz for the configuration of the suspension system described previously.

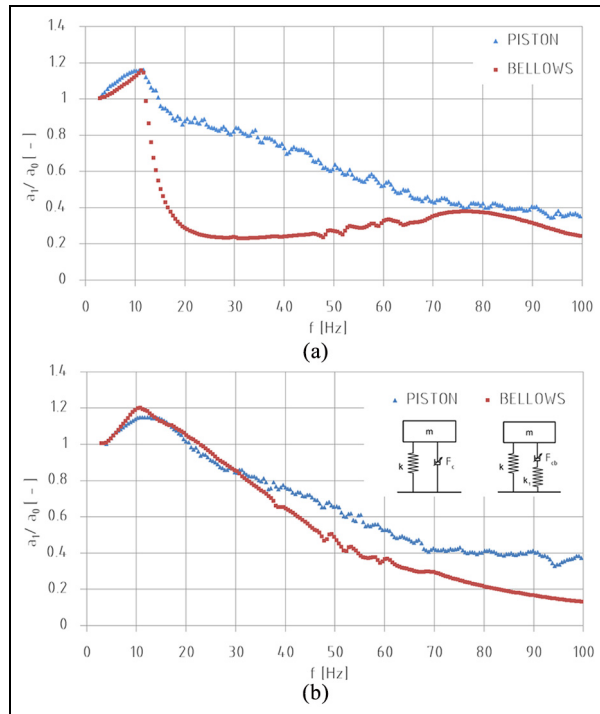


Figure 11. Comparison of transfer ratios: (a) adaptive-passive $l = 1 \text{ A}$ ($f \leq 12 \text{ Hz}$) and $l = 0 \text{ A}$ ($f > 12 \text{ Hz}$); (b) passive $l = 0.5 \text{ A}$.

The improvement of the transfer ratio in the isolation area caused by an elastically connected damper occurs in the case of high velocity and small stroke of the damper when the damping force F_{cb} is higher than the force necessary for compression of spring with stiffness k_1 . The sprung mass oscillates on two springs, the total stiffness of which is the sum $k + k_1$ that improves the isolation properties of the system.

Benefits of the elastically connected dampers are well known and often used, for example, in automotive dampers which have elastic parts (silent blocks) in eye mounts because of vibration elimination at high frequencies and low strokes. The MR damper with bellows works similarly; however, the elasticity is given especially by volumetric stiffness of the bellows, more precisely by its projection into axial direction—pressure thrust stiffness. The selection of suitable bellows is very important for the MR damper design because it affects the ratio N and thus the transfer function of the suspension (equation (5)). A method of the pressure thrust stiffness determination based on the bellows dimensions uses finite element analysis (FEA) and is described in our previous study.²⁹

Conclusion

The frictionless MR damper with bellows has been tested in this study and compared with the original MR

damper with a piston. The bellows unit was designed to eliminate friction by replacement of the piston and piston rod sealings by static seals of bellows. The measurement of force–velocity dependency proved that the force caused by friction in the damper has a significant impact on the dynamic force range of such device. An increase of the dynamic force range for the frictionless damper is more than 100% for damper velocity lower than 0.08 m/s . This should significantly improve the quality of damping using a semi-active algorithm.⁵

The adaptive-passive damping control was used to compare the behaviour of the frictionless MR damper and the original MR damper with a piston in the same suspension. The transfer ratio of the suspension with a frictionless MR damper was lower in the whole frequency range in comparison with the transfer ratio of the suspension with the original MR damper with a piston. A new design of the damper with bellows can be considered as elastically connected. This results in a lower transfer ratio for high frequencies in comparison with the transfer ratio of the damper with a piston which is considered as rigidly connected.

The dynamic force range together with the response time of the MR damper is the most important parameter limiting the performance of suspension systems controlled by semi-active algorithms. It can be concluded that the use of the bellows unit instead of the piston unit brings about a promising improvement of suspension quality in semi-active suspension systems.



Declaration of conflicting interests

The author(s) declared no potential conflicts of interest with respect to the research, authorship and/or publication of this article.

Funding

The author(s) disclosed receipt of the following financial support for the research, authorship and/or publication of this article: This study was supported by the kind sponsorship of various grants and numerous agencies. This study was especially supported through GAČR 17-10660J, GAČR 17-26162S and FSI-S-17-4428.

ORCID iDs

Ondřej Macháček  <https://orcid.org/0000-0003-4720-6375>
Zbyněk Strecker  <https://orcid.org/0000-0002-1598-487X>

References

1. Housner GW, Bergman LA, Caughey TK, et al. Structural control: past, present, and future. *J Eng Mech* 1997; 123: 897–971.
2. Gaul L, Hurlebaus S, Wornitzer J, et al. Enhanced damping of lightweight structures by semi-active joints. *Acta Mech* 2008; 195: 249–261.

3. Symans MD and Constantinou MC. Semi-active control systems for seismic protection of structures: a state-of-the-art review. *Eng Struct* 1999; 21: 469–487.
4. Ding Y, Zhang L, Zhu HT, et al. A new magnetorheological damper for seismic control. *Smart Mater Struct* 2013; 22: 115003.
5. Yang G, Spencer BF Jr, Carlson JD, et al. Large-scale MR fluid dampers: modeling and dynamic performance considerations. *Eng Struct* 2002; 24: 309–323.
6. Guo CY, Gong XL, Zong LH, et al. Twin-tube- and bypass-containing magneto-rheological damper for use in railway vehicles. *Proc IMechE, Part F: J Rail and Rapid Transit* 2015; 229: 48–57.
7. Ichwan B, Mazlan SA, Imaduddin F, et al. Development of a modular MR valve using meandering flow path structure. *Smart Mater Struct* 2016; 25: 037001.
8. Roupec J, Mazurek I, Strecker Z, et al. The behavior of the MR fluid during durability test. *J Phys Conf Ser* 2013; 412: 012024.
9. Mazurek I, Roupec J, Klapka M, et al. Load and rheometric unit for the test of magnetorheological fluid. *Mechanica* 2013; 48: 631–641.
10. Sun JQ, Jolly M and Norris MA. Passive, adaptive and active tuned vibration absorbers – a survey. *J Mech Design* 1995; 117: 234–242.
11. Snowdon JC. *Vibration and shock in damped mechanical systems*. New York: John Wiley, 1968.
12. Franchek MA, Ryan MW and Bernhard RJ. Adaptive passive vibration control. *J Sound Vib* 1996; 189: 565–585.
13. Liu Y, Waters TP and Brennan MJ. A comparison of semi-active damping control strategies for vibration isolation of harmonic disturbances. *J Sound Vib* 2005; 280: 21–39.
14. Koo JH, Goncalves FD and Ahmadian M. A comprehensive analysis of the response time of MR dampers. *Smart Mater Struct* 2006; 15: 351–358.
15. Mass J and Gueth D. Experimental investigation of the transient behavior of MR fluids. In: *ASME conference on smart materials, adaptive structures and intelligent systems*, Scottsdale, AZ, 18–21 September 2011, pp.229–238. New York: ASME.
16. Strecker Z, Roupec J, Mazurek I, et al. Design of magnetorheological damper with short time response. *J Intel Mat Syst Str* 2015; 26: 1951–1958.
17. Nguyen QH and Choi SB. Optimal design of a vehicle magnetorheological damper considering the damping force and dynamic range. *Smart Mater Struct* 2009; 18: 015013.
18. Bai XX and Wereley NM. A fail-safe magnetorheological energy absorber for shock and vibration isolation. *J Appl Phys* 2014; 115: 17B535.
19. Cvek M, Mrlik M, Ilcikova M, et al. A facile controllable coating of carbonyl iron particles with poly(glycidyl methacrylate): a tool for adjusting MR response and stability properties. *J Mater Chem C* 2015; 3: 4646–4656.
20. Wang Q, Ahmadian M and Chen Z. A novel double-piston magnetorheological damper for space truss structures vibration suppression. *Shock Vib* 2014; 2014: 864765.
21. Kubik M, Machacek O, Strecker Z, et al. Design and testing of magnetorheological valve with fast force response time and great dynamic force range. *Smart Mater Struct* 2017; 26: 047002.
22. Harris CM and Piersol AG. *Harris' shock and vibration handbook*. New York: McGraw-Hill, 2002.
23. Igers W, Papatheodorou T and Hannifin P. Low-friction seals lead to high machine efficiency. *Hydraulics & Pneumatics*, 12 September, <http://hydraulicspneumatics.com/200/TechZone/Seals/Article/False/86292/TechZone-Seals> (2010, accessed 13 September 2010).
24. Heipl O and Murrenhoff H. Friction of hydraulic rod seals at high velocities. *Tribol Int* 2015; 85: 66–73.
25. Lee DO, Park GY and Han JH. Experimental study on on-orbit and launch environment vibration isolation performance of a vibration isolator using bellows and viscous fluid. *Aerosp Sci Technol* 2015; 45: 1–9.
26. Seong MS, Choi SB and Kim CH. Damping force control of frictionless MR damper associated with hysteresis modeling. *J Phys Conf Ser* 2013; 412: 012044.
27. Davis P, Cunningham D and Harrell J. Advanced 1.5 Hz passive viscous isolation system. *Am Inst Aeronaut Astronaut* 1994; 35: 2655–2666.
28. Brennan MJ, Carrella A, Waters TP, et al. On the dynamic behaviour of a mass supported by a parallel combination of a spring and an elastically connected damper. *J Sound Vib* 2008; 309: 823–837.
29. Machacek O, Kubik M, Strecker Z, et al. Axial and pressure thrust stiffness of metal bellows for vibration isolators. *MATEC Web Conf* 2018; 153: 06001.